Theoretical Population Biology 90 (2013) 91–103

Contents lists available at ScienceDirect

Theoretical Population Biology

journal homepage: www.elsevier.com/locate/tpb

Characteristics of the variance effective population size over time using an age structured model with variable size

Fredrik Olsson [a,*], Ola Hössjer [a], Linda Laikre [b], Nils Ryman [b]

[a] Department of Mathematics, Div. of Mathematical Statistics, Stockholm University, Stockholm, Sweden
[b] Department of Zoology, Div. of Population Genetics, Stockholm University, Stockholm, Sweden

ARTICLE INFO

Article history:
Received 1 April 2013
Available online 8 October 2013

Keywords:
Variance effective population size
Fluctuating size of age classes
Overlapping generations
Temporal method

ABSTRACT

The variance effective population size (N_{eV}) is a key concept in population biology, because it quantifies the microevolutionary process of random genetic drift, and understanding the characteristics of N_{eV} is thus of central importance. Current formulas for N_{eV} for populations with overlapping generations weight age classes according to their reproductive values (i.e. reflecting the contribution of genes from separate age classes to the population growth) to obtain a correct measure of genetic drift when computing the variance of the allele frequency change over time. In this paper, we examine the effect of applying different weights to the age classes using a novel analytical approach for exploring N_{eV}. We consider a haploid organism with overlapping generations and populations of increasing, declining, or constant expected size and stochastic variation with respect to the number of individuals in the separate age classes. We define N_{eV}, as a function of how the age classes are weighted, and of the span between the two points in time, when measuring allele frequency change. With this model, time profiles for N_{eV} can be calculated for populations with various life histories and with fluctuations in life history composition, using different weighting schemes. We examine analytically and by simulations when N_{eV}, using a weighting scheme with respect to reproductive contribution of separate age classes, accurately reflect the variance of the allele frequency change due to genetic drift over time. We show that the discrepancy of N_{eV}, calculated with reproductive values as weights, compared to when individuals are weighted equally, tends to a constant when the time span between the two measurements increases. This constant is zero only for a population with a constant expected population size. Our results confirm that the effect of ignoring overlapping generations, when empirically assessing N_{eV} from allele frequency shifts, gets smaller as the time interval between samples increases. Our model has empirical applications including assessment of (i) time intervals necessary to permit ignoring the effect of overlapping generations for N_{eV} estimation by means of the temporal method, and (ii) effects of life table manipulation on N_{eV} over varying time periods.

1. Introduction

The concept of effective population size (N_e) was introduced by Wright (1931) and is of key importance in population biology. Wright defined N_e as "the number of breeding individuals in an idealized population that would show the same amount of dispersion of allele frequencies under random genetic drift or the same amount of inbreeding as the population under consideration". Several closely related variants have since then been developed and studied, such as the variance, inbreeding, coalescence, and eigenvalue effective population size (Crow and Denniston, 1988; Wang and Caballero, 1999; Waples, 2002; Ewens, 2004; Sagitov and Jagers, 2005; Sjödin et al., 2005; Charlesworth, 2009; Hössjer, 2011). Important applications of N_e include for instance understanding of microevolutionary dynamics (Ewens, 2004), determining minimum viable populations in conservation biology (Franklin, 1980; Allendorf and Ryman, 2002; Jamieson and Allendorf, 2012), and designing and monitoring artificial breeding programs (Lande and Barrowclough, 1987).

In this paper, we focus on the variance effective population size (N_{eV}), which is the size of an ideal, Wright–Fisher model, (Wright, 1931) population with the same variance of allele frequency change of a neutral gene, as the studied population. For a haploid Wright–Fisher population of size N_{eV} with an initial allele frequency p, this variance is $p(1-p)(1-(1-1/N_{eV})^t)$ after t time steps (Nei, 1975, Section 5.1.2). Deviations from ideal conditions, such as separate sexes of unequal ratio, varying population size or other than binomial distribution of progeny will affect the variance of the allele frequency change. Further, introducing age structured populations will complicate the calculation of N_{eV}. In one sense it is most natural to assign the same weight to each

* Corresponding author.
E-mail address: fredriko@math.su.se (F. Olsson).

0040-5809/$ – see front matter
http://dx.doi.org/10.1016/j.tpb.2013.09.014

Table 1
List of notation used in the paper.

Notation	Definition
b_i	Mean number of offspring for an individual in age class i
l_i	Probability that an individual survives to age class i
s_i	Probability that an individual in age class i survives to age class $i+1$
$\boldsymbol{G}_t$	Projection matrix of vital rates for $\boldsymbol{Z}$
$\boldsymbol{H}_t$	Projection matrix of vital rates for $\boldsymbol{Y}$
$\boldsymbol{g}$	Expected projection matrix
$\boldsymbol{\delta}_t$	Matrix of serially uncorrelated demographic noise for $\boldsymbol{Z}$-process
λ	Multiplicative growth rate and largest eigenvalue of $\boldsymbol{g}$
$\boldsymbol{u}$	Vector of the approximate equilibrium age distribution for $\boldsymbol{Z}$, $\boldsymbol{Y}$ and $\boldsymbol{N}$
$\boldsymbol{v}$	Vector proportional to the reproductive values
$\boldsymbol{c}$	Arbitrary vector of age class weights normalized such that $\boldsymbol{cu}=1$
$p_t^{\boldsymbol{c}}$	The population allele frequency at time t when age classes are weighted with $\boldsymbol{c}$
$\boldsymbol{N}_t$	Vector containing number of individuals in all age classes
$N_t^{\boldsymbol{c}}$	Population size when age classes are weighted by $\boldsymbol{c}$
$\boldsymbol{Z}_t$	Vector containing number of individuals with the specified allele in all age classes
$Z_t^{\boldsymbol{c}}$	Number of individuals with the specified allele when age classes are weighted by $\boldsymbol{c}$
$\boldsymbol{Y}_t$	Vector containing number of individuals without the specified allele in all age classes
$Y_t^{\boldsymbol{c}}$	Number of individuals without the specified allele when age classes are weighted by $\boldsymbol{c}$
ϵ_t	Vector of deviations from the asymptotic proportions $\boldsymbol{u}$ of the number of alleles in each age class
τ	Time between measurements when applying the temporal method for assessing N_{eV}. One time unit represents the age difference of two successive age classes
N_{eV}	Variance effective population size
$\sigma^2_{d,\boldsymbol{c}}(\tau)$	Demographic variance measured over τ time steps when $\boldsymbol{c}$ is used as the weight vector
$N^{\boldsymbol{c}}_{eV,t}(\tau)$	Variance effective population size measured over τ time steps when $\boldsymbol{c}$ is used as the weight vector
T	Generation time i.e. mean age of parents of newborns
$\boldsymbol{V}$	Covariance matrix which quantifies deviations of the allele frequencies in age classes from numbers proportional to $\boldsymbol{u}$
$\Delta_{\boldsymbol{c}}(\tau)$	Relative discrepancy of $N^{\boldsymbol{c}}_{eV,t}(\tau)$ compared to $N^{\boldsymbol{v}}_{eV,t}(\tau)$.

individual as this gives the actual allele frequencies. However, with such uniform weights the variance of the allele frequency change will initially fluctuate, and only after a number of time steps will these fluctuations settle so that the variance increases at a steady rate as for the Wright–Fisher model (Hill, 1979). From an evolutionary perspective these initial fluctuations will not represent true genetic drift; rather, allele frequency change will be largely an effect of the age structure (Jorde and Ryman, 1995).

Expressions for the variance effective population size for haploids with overlapping generations have previously been derived assuming fixed number of individuals in each age class (Felsenstein, 1971; Hill, 1972, 1979). Engen et al. (2005a) analyzed populations with fluctuating population size based on asymptotics for large populations and diffusion approximations (Tuljapurkar, 1982; Lande and Orzack, 1988; Lande et al., 2003). All these models aim to eliminate the initial fluctuations and describe the asymptotic variance of allele frequency change by considering the variance between two points in time. Instead of using uniform weights where all individuals are weighted equally, these formulas are only valid when each individual is weighted according to its age class reproductive value (Fisher, 1958).

In this paper we derive a general expression for N_{eV} as a function of how individuals are weighted. As opposed to previous work we show that the allele frequency change can be written as a sum of two terms, one due to genetic drift and one due to random variation of the demographic distribution of allele frequencies. Only the genetic drift has previously been treated since the other term vanishes when reproductive weights are used. We consider the variance of the allele frequency change between two measurements separated by an arbitrary time span. We also allow the total population size, as well as the sizes of the age classes, to fluctuate. Hence, N_{eV} can be plotted analytically as a function of the length of the time interval between the two points of allele frequency assessment, the weighting scheme and the population growth scenario. We study N_{eV} with uniform as well as reproductive weights and examine how well these two weighting schemes coincide.

Our theoretical exploration of N_{eV} is of relevance for empirical situations; the most common method of assessing rate of genetic drift in natural populations is by estimating N_{eV} from temporal changes of allele frequencies (Waples, 1989; Wang and Whitlock, 2003). Since most natural populations have overlapping generations, it is important to investigate the behavior of the temporal method under such conditions.

The paper is structured as follows: In the first section we define the population genetic model and describe the temporal dynamics of the system. Next, we consider the amount of allele frequency change between two consecutive points in time and provide expressions for N_{eV} and the demographic variance (Engen et al., 2005b), which quantifies random variation among individuals in reproduction and survival. Then we generalize these ideas by considering the allele frequency change between two time points separated by several time steps, and give generalized expressions for the demographic variance and N_{eV}. In Section 5 we perform a simulation study in order to check the accuracy of these expressions. In Section 6 we present formulas for calculating the discrepancy of the asymptotic N_{eV} for reproductive and uniform (or other) weights. Mathematical derivations are collected in Appendices A–G, and Table 1 summarizes the most important notation.

2. Population genetic model

Consider a population of haploid individuals divided into n age classes and assume that a certain selectively neutral biallelic gene (locus) is segregating in the population. The age distribution of the individuals with one of the alleles at time t is described using the column vector $\boldsymbol{Z}_t = (Z_{t,0},\ldots,Z_{t,n-1})'$ where $Z_{t,i}$ is the total number of copies of the allele within age class i and $'$ denotes matrix transposition. The age distribution of the individuals without the specified allele at time t is described using the vector $\boldsymbol{Y}_t = (Y_{t,0},\ldots,Y_{t,n-1})'$ where $Y_{t,i}$ is the total number of copies of the non-specified allele within age class i. Hence, the total population is described by the vector $\boldsymbol{N}_t = (N_{t,0},\ldots,N_{t,n-1})' = (Z_{t,0}+Y_{t,0},\ldots,Z_{t,n-1}+Y_{t,n-1})'$ where $N_{t,i}$ is the number of individuals in age class i at time t.

Each individual in generation t and age class i independently gives birth to a number of progeny with mean b_i and variance σ_i^2,

and with probability s_i it survives to the next age class. Moreover, we allow for a correlation ρ_i between the number of progeny and survival of a parent.

The time dynamics of both alleles is described using matrix population models (cf. Caswell, 2001). Since we assume a selectively neutral gene and since the individuals are haploid, the dynamics of both alleles' subpopulations can be described by the matrix recursion formulas

$$\begin{aligned} \boldsymbol{Z}_{t+1} &= \boldsymbol{G}_t \boldsymbol{Z}_t, \\ \boldsymbol{Y}_{t+1} &= \boldsymbol{H}_t \boldsymbol{Y}_t, \end{aligned}$$

where $\boldsymbol{G}_t = (G_{t,ij})$ and $\boldsymbol{H}_t = (H_{t,ij})$ are $n \times n$ projection matrices of vital rates, whose nonzero components are listed in (A.1) and (A.2) in Appendix A. Write

$$\begin{aligned} \boldsymbol{G}_t &= \boldsymbol{g} + \boldsymbol{\delta}_t, \\ \boldsymbol{H}_t &= \boldsymbol{g} + \boldsymbol{d}_t, \end{aligned} \tag{1}$$

where $\boldsymbol{g} = E(\boldsymbol{G}_t) = E(\boldsymbol{H}_t) = (g_{ij})$ is the expected projection or Leslie matrix (Leslie, 1945), with nonzero elements $g_{0i} = b_i$ and $g_{i+1,i} = s_i$ along the first row and subdiagonal respectively. The zero mean matrices $\boldsymbol{\delta}_t = (\delta_{t,ij})$ and $\boldsymbol{d}_t = (d_{t,ij})$ represent serially uncorrelated demographic noise.

From $\boldsymbol{g}$, a number of important quantities can be derived. The multiplicative growth rate of the population is the largest eigenvalue of $\boldsymbol{g}$ which we denote λ. It follows from the Perron–Frobenius Theorem that $\boldsymbol{g}$ has a unique largest and real-valued eigenvalue since $\boldsymbol{g}$ has non-negative entries and is irreducible and aperiodic. The reproductive values $\boldsymbol{v} = (v_0, \ldots, v_{n-1})$, which quantify the expected contribution to population growth of all age classes, are proportional to the left eigenvector corresponding to eigenvalue λ. The right eigenvector $\boldsymbol{u} = (u_0, \ldots, u_{n-1})'$ corresponding to λ is proportional to the approximate equilibrium age distribution. For convenience, $\boldsymbol{u}$ and $\boldsymbol{v}$ are normalized so that

$$\sum_{i=0}^{n-1} u_i = 1$$

and

$$\sum_{i=0}^{n-1} v_i u_i = 1 \tag{2}$$

hold. The latter normalization implies that on average, the number of descendants of an age class i individual τ time points later is $\lambda^\tau v_i$, provided τ is large enough. Explicit formulas for both $\boldsymbol{u}$ and $\boldsymbol{v}$ are given in Appendix B.

Let $\boldsymbol{c} = (c_0, \ldots, c_{n-1})$ be an arbitrary vector of weights satisfying $\boldsymbol{cu} = 1$ and let $Z_t^{\boldsymbol{c}} = \boldsymbol{c}\boldsymbol{Z}_t$ be the weighted sum of the components of $\boldsymbol{Z}_t$. Then, $Z_t^{\boldsymbol{1}} = \boldsymbol{1}\boldsymbol{Z}_t = \sum_{i=0}^{n-1} Z_{t,i}$ denotes the total number of individuals with the specified allele at time t, where $\boldsymbol{1}$ is a row vector of ones, and $N_t^{\boldsymbol{1}} = \boldsymbol{1}\boldsymbol{N}_t = \sum_{i=0}^{n-1} N_{t,i}$ denotes the total population size at time t. With a large population and small variances of the vital rates in (1), it follows that the age distribution of both the total population and the allele subpopulation reach the approximate equilibrium limit $\boldsymbol{u} = (u_0, \ldots, u_{n-1})'$ after some iterations, so that

$$\begin{aligned} \boldsymbol{Z}_t &\approx Z_t^{\boldsymbol{1}} \boldsymbol{u}, \\ \boldsymbol{N}_t &\approx N_t^{\boldsymbol{1}} \boldsymbol{u}, \end{aligned} \tag{3}$$

and

$$\begin{aligned} \boldsymbol{Z}_{t+1} &\approx \lambda \boldsymbol{Z}_t, \\ \boldsymbol{N}_{t+1} &\approx \lambda \boldsymbol{N}_t. \end{aligned} \tag{4}$$

For further calculations, we need to provide a more detailed description of the absolute frequencies of the two alleles than provided by (3). It will be convenient to divide the processes $\boldsymbol{Z}_t$ and $\boldsymbol{Y}_t$ into two parts. Let

$$\begin{aligned} \boldsymbol{Z}_t &= Z_t \boldsymbol{u} + \epsilon_t, \\ \boldsymbol{Y}_t &= Y_t \boldsymbol{u} + \varepsilon_t, \end{aligned} \tag{5}$$

where ϵ_t is the deviation from the asymptotic proportions $\boldsymbol{u}$ of individuals with the specified allele in each age class, $Z_t = Z_t^{\boldsymbol{v}} = \boldsymbol{v}\boldsymbol{Z}_t$ is the number of individuals with the specified allele when age classes are weighted by $\boldsymbol{v}$ and in analogous way, ε_t and Y_t are defined.

3. Effective population size

In order to derive an expression for the variance effective population size we need to quantify the change in allele frequencies for alleles measured at two consecutive time points. First, define the allele frequency of the population

$$p_t^{\boldsymbol{c}} = \frac{Z_t^{\boldsymbol{c}}}{N_t^{\boldsymbol{c}}} = \frac{\boldsymbol{c}\boldsymbol{Z}_t}{\boldsymbol{c}\boldsymbol{N}_t},$$

as a weighted average of the allele frequencies of the age classes. Then, let the variance of the allele frequency change $E((p_{t+1}^{\boldsymbol{c}} - p_t^{\boldsymbol{c}})^2 | N_t^{\boldsymbol{c}}, p_t^{\boldsymbol{c}})$ equal the variance of allele frequency change for a Wright–Fisher model $p_t^{\boldsymbol{c}}(1-p_t^{\boldsymbol{c}})(1-(1-1/N_{eV,t}^{\boldsymbol{c}})^{1/T})$. The fraction $1/T$ corresponds to one time step where T is defined as the mean age of parents of newborns when a multiplicative growth rate of the drift is assumed (Luikart et al., 1999; Engen et al., 2005a). We have that

$$\begin{aligned} \frac{1}{N_{eV}^{\boldsymbol{c}}} &= 1 - \left(1 - \frac{E((p_{t+1}^{\boldsymbol{c}} - p_t^{\boldsymbol{c}})^2 | N_t^{\boldsymbol{c}}, p_t^{\boldsymbol{c}})}{p_t^{\boldsymbol{c}}(1-p_t^{\boldsymbol{c}})}\right)^T \\ &\approx \frac{TE((p_{t+1}^{\boldsymbol{c}} - p_t^{\boldsymbol{c}})^2 | N_t^{\boldsymbol{c}}, p_t^{\boldsymbol{c}})}{p_t^{\boldsymbol{c}}(1-p_t^{\boldsymbol{c}})}. \end{aligned} \tag{6}$$

Based on Taylor expansions, valid for low levels of stochasticity in vital rates, we show that

$$E\left((p_{t+1}^{\boldsymbol{c}} - p_t^{\boldsymbol{c}})^2 | N_t^{\boldsymbol{c}}, p_t^{\boldsymbol{c}}\right) \approx \frac{\sigma_{d,\boldsymbol{c}}^2 p_t^{\boldsymbol{c}}(1-p_t^{\boldsymbol{c}})}{N_t^{\boldsymbol{c}}}, \tag{7}$$

where

$$\begin{aligned} \sigma_{d,\boldsymbol{c}}^2 &= \lambda^{-2}(Z_t^c)^{-1} E((Z_{t+1}^{\boldsymbol{c}} - \lambda Z_t^{\boldsymbol{c}})^2 | Z_t^{\boldsymbol{c}}) \\ &\approx \lambda^{-2} Z_t E((\boldsymbol{c}\boldsymbol{\delta}_t\boldsymbol{u})^2 | Z_t) + \lambda^{-2} Z_t^{-1} E((\boldsymbol{c}(\boldsymbol{g} - \lambda \boldsymbol{I})\epsilon_t)^2 | Z_t) \end{aligned} \tag{8}$$

is the demographic variance and $\boldsymbol{I}$ is the identity matrix of order n. The first equality of (8) is a definition (see Appendix C), and the approximation in the second step is motivated in Appendix D. Eq. (8) reveals that the magnitude of allele frequency change in the whole population, as quantified by $\sigma_{d,\boldsymbol{c}}^2$, can be decomposed into two parts. The first term corresponds to the genetic drift of the whole population and the second term reflects random variation of the demographic distribution (between age classes) of allele frequencies. Insertion of (7) into (6) yields

$$N_{eV,t}^{\boldsymbol{c}} = \frac{N_t^{\boldsymbol{c}}}{T\sigma_{d,\boldsymbol{c}}^2}. \tag{9}$$

In order to get a more explicit expression for $\sigma_{d,\boldsymbol{c}}^2$, it is convenient to introduce the matrix

$$\boldsymbol{C}_j = Z_{tj} \mathrm{Cov}\left(\boldsymbol{\delta}_{tj}\right), \tag{10}$$

where $\boldsymbol{\delta}_{tj}$ is column j of $\boldsymbol{\delta}_t$ with nonzero elements δ_{tj0} and $\delta_{t,j+1,j}$. Reproduction is assumed to be independent between age classes,

so that the columns $\boldsymbol{\delta}_{t0}, \ldots, \boldsymbol{\delta}_{t,n-1}$ of $\boldsymbol{\delta}_t$ are independent random vectors. Then

$$\boldsymbol{\Sigma} = \sum_{j=0}^{n-1} u_j \boldsymbol{C}_j \approx Z_t \mathrm{Cov}(\boldsymbol{\delta}_t \boldsymbol{u}) \tag{11}$$

where the last approximation is exact when $Z_{tj} = Z_t u_j$ for $j = 0, \ldots, n-1$. We show in Appendix D that (8) can be rewritten as

$$\sigma^2_{d,\boldsymbol{c}} \approx \lambda^{-2} \boldsymbol{c}\boldsymbol{\Sigma}\boldsymbol{c}' + \boldsymbol{c}(\boldsymbol{g}\lambda^{-1} - \boldsymbol{I})\boldsymbol{V}(\boldsymbol{g}\lambda^{-1} - \boldsymbol{I})'\boldsymbol{c}', \tag{12}$$

where $\boldsymbol{V}$, which is described in Appendices D and F, is a covariance matrix that approximates $\mathrm{Cov}(\epsilon_t|Z_t)/Z_t$ and quantifies, for each of the two alleles, deviations of the age class distribution from $\boldsymbol{u}$. The first part of (12) depends on demographic parameters only at time t. However, since $\boldsymbol{V}$ is a convergent sum of terms which depends on the past, the second part requires that the demographic parameters have been constant prior to time t. In practice, this means that using (9) for prediction of the effective populations size imposes the condition that the demographic parameters prior time point t have been constant.

By weighting individuals according to their age class reproductive value the last term in (8) and (12) equals zero. Hence, in this case no assumption on the demographic parameters prior to time t needs to be made. In Appendix E we also show that, for these weights, we end up with the same expression for the demographic variance as in Engen et al. (2005a).

4. Effective population size over longer time intervals

In this section we derive an expression for the variance effective population size based on the change in allele frequencies between time t and $t+\tau$. Let $\sigma^2_{d,\boldsymbol{c}}(\tau)$ be the demographic variance when looking τ time steps ahead in time. We show that

$$\begin{aligned}\sigma^2_{d,\boldsymbol{c}}(\tau) &= \frac{1}{\lambda^{2\tau} Z_t^{\boldsymbol{c}}} E\left((Z_{t+\tau}^{\boldsymbol{c}} - \lambda^\tau Z_t^{\boldsymbol{c}})^2 | Z_t^{\boldsymbol{c}}\right) \\ &\approx \lambda^{-\tau-1}\boldsymbol{c}\left(\sum_{r=0}^{\tau-1}\lambda^{-r}\boldsymbol{g}^r\boldsymbol{\Sigma}(\boldsymbol{g}^r)'\right)\boldsymbol{c}' \\ &\quad + \boldsymbol{c}(\boldsymbol{g}^\tau\lambda^{-\tau} - \boldsymbol{I})\boldsymbol{V}(\boldsymbol{g}^\tau\lambda^{-\tau} - \boldsymbol{I})'\boldsymbol{c}'\end{aligned} \tag{13}$$

and

$$E\left((p_{t+\tau}^{\boldsymbol{c}} - p_t^{\boldsymbol{c}})^2 | p_t^{\boldsymbol{c}}, N_t^{\boldsymbol{c}}\right) \approx \frac{\sigma^2_{d,\boldsymbol{c}}(\tau) p_t^{\boldsymbol{c}}(1-p_t^{\boldsymbol{c}})}{N_t^{\boldsymbol{c}}}. \tag{14}$$

The first equality of (13) is a definition (see Appendix C), and the approximation in the second step is motivated in Appendix D. As in (8), the allele frequency change can be decomposed into one genetic drift part and another part that reflects random variation between age classes in terms of allele frequencies. Generalizing (6), we have that the reciprocal of the variance effective population size equals

$$\begin{aligned}\frac{1}{N_{eV}^{\boldsymbol{c}}(\tau)} &= 1 - \left(1 - \frac{E((p_{t+\tau}^{\boldsymbol{c}} - p_t^{\boldsymbol{c}})^2 | N_t^{\boldsymbol{c}}, p_t^{\boldsymbol{c}})}{p_t^{\boldsymbol{c}}(1-p_t^{\boldsymbol{c}})}\right)^{T/\tau} \\ &\approx \frac{TE((p_{t+\tau}^{\boldsymbol{c}} - p_t^{\boldsymbol{c}})^2 | p_t^{\boldsymbol{c}}, N_t^{\boldsymbol{c}})}{\tau p_t^{\boldsymbol{c}}(1-p_t^{\boldsymbol{c}})}\end{aligned} \tag{15}$$

as a function of τ. For a large population, by combining (13)–(15), we have that

$$\begin{aligned}\frac{1}{N_{eV,t}^{\boldsymbol{c}}(\tau)} \approx \frac{T}{\tau}\Bigg(&\frac{1}{N_t^{\boldsymbol{c}}}\lambda^{-\tau-1}\boldsymbol{c}\left(\sum_{r=0}^{\tau-1}\lambda^{-r}\boldsymbol{g}^r\boldsymbol{\Sigma}(\boldsymbol{g}^r)'\right)\boldsymbol{c}' \\ &+ \frac{1}{N_t^{\boldsymbol{c}}}\boldsymbol{c}(\boldsymbol{g}^\tau\lambda^{-\tau} - \boldsymbol{1})\boldsymbol{V}(\boldsymbol{g}^\tau\lambda^{-\tau} - \boldsymbol{1})'\boldsymbol{c}'\Bigg).\end{aligned} \tag{16}$$

If we let $\boldsymbol{c} = \boldsymbol{v}$, the second term in (16) vanishes and the reciprocal of the variance effective population size (16) simplifies considerably, to

$$\frac{1}{N_{eV,t}(\tau)} \approx \frac{T}{\tau}\lambda^{-2}\boldsymbol{v}\boldsymbol{\Sigma}\boldsymbol{v}'\sum_{r=0}^{\tau-1}\frac{1}{N_t^{\boldsymbol{v}}\lambda^r}. \tag{17}$$

The variance effective population size, based on the genetic drift between time t and $t+\tau$, is then the harmonic mean of the effective population sizes $N_t^{\boldsymbol{v}}\lambda^r/(\lambda^{-2}\boldsymbol{v}\boldsymbol{\Sigma}\boldsymbol{v}')$ at time $t+r$ where $r = 0, \ldots, \tau-1$, multiplied by a factor that depends on the generation time T. Our expression (17) is similar to the expression for the effective population size, both with a deterministic varying population (Crow and Kimura, 1970, Eq. 7.6.3.34) and with a stochastic varying population (Engen et al., 2005a, Eq. 14).

A more intuitive reason for why the second term of (16) vanishes for reproductive weights $\boldsymbol{v}$, is that the deviations ϵ_t and ε_t from the age proportions $\boldsymbol{u}$, are both orthogonal to $\boldsymbol{v}$. Therefore, for reproductive weights, the system can be analyzed as if age proportions $\boldsymbol{u}$ were fixed, see Appendix D.

As in the previous section, if $\boldsymbol{c} \neq \boldsymbol{v}$, the effective population size at time t will depend on the demographic history before t. Hence, prediction of the effective population size according to (16) requires constant demographic parameters prior time t for all weights except for $\boldsymbol{c} = \boldsymbol{v}$.

5. Simulations

Waples and Yokota (2007) performed extensive simulations in order to study the bias of the standard temporal method estimate of the effective population size when violating the assumption of non-overlapping generations. Their conclusion was that in order to obtain an unbiased estimate of the effective population size under such conditions, the allele frequencies in each age class should be weighted by the corresponding reproductive value in agreement with the proposal of Felsenstein (1971). It has also been observed that the bias for the unweighted estimate is reduced when the time between measurements is increased (Jorde and Ryman, 1995; Waples and Yokota, 2007).

In this section, we present results of computer simulations of the allele frequency change used to validate the formula for the effective population size (15). Following Waples and Yokota (2007), we choose to model three species with different survival schedules, humans (Felsenstein, 1971), white-crowned sparrows (Baker et al., 1981), and barnacles (Connell, 1970). For each species, we modified the published data by multiplying the expected number of births in each age class by a constant in order to adjust λ and obtain a stable, a growing, and a decreasing growth scenario. For the barnacle data, we increased the survival probability by a factor 10 compared to the published data to obtain values comparable to those of Waples and Yokota (2007). In our simulations we did not include the last age class in the published data for humans, because that age class consists of old individuals that do not reproduce. The exclusion of this age class does not affect the effective population size when $\boldsymbol{c} = \boldsymbol{v}$ since its reproductive number equals zero.

We assume that the number of progeny is Poisson distributed for all scenarios, hence $\sigma_i^2 = b_i$, and that covariance between survival and number of progeny is zero, i.e. $\rho_i = 0$. Time is measured in years for sparrows and barnacles, and in 5-year periods for humans in agreement with the published data. We also assume that individuals are haploid although the published data refers to the female part of the populations. The life history parameters used in the simulations are presented in Table 2.

For each species and scenario, we simulate 120 time steps and repeat the procedure 10 000 times. In each time step, we simulate the number of progeny and survival of each individual according

Table 2

Life table data for three different scenarios of humans, sparrows and barnacles where b_i is the mean number of progeny for an individual in age class i, $l_i = \prod_{j=0}^{i-1} s_j$ is the probability for an individual to survive to age class i and s_i the probability that an individual in age class i survives to age class $i+1$. The expected growth rate λ is given for the different scenarios and N_0 is the population size at time 0 when the allele frequency is measured for the first time. Each age class represents 5 years for humans and 1 year for barnacles and sparrows. Hence, the generation time in years for humans is $5T$.

Age class	Human				Sparrow				Barnacle			
		Stable	Growing	Decreasing		Stable	Growing	Decreasing		Stable	Growing	Decreasing
	l_i	b_i	b_i	b_i	l_i	b_i	b_i	b_i	l_i	b_i	b_i	b_i
0	1.0	0	0	0	1.0	0	0	0	1.0	0	0	0
1	0.97891	0	0	0	0.167	3.018	3.142	2.8278	0.00062	358.6	362.2	340.7
2	0.97754	0.0172	0.0208	0.0149	0.083	3.202	3.333	2.9997	0.00034	678.2	685.0	644.4
3	0.97486	0.2905	0.3515	0.2511	0.048	3.416	3.556	3.2004	0.00020	904.2	913.4	859.3
4	0.97179	0.3435	0.4157	0.2969	0.012	3.602	3.750	3.3750	0.00016	989.9	1000	940.7
5	0.96841	0.2150	0.2602	0.1859	0.006	3.842	4.000	3.6000	0.00011	989.9	1000	940.7
6	0.96841	0.1138	0.1377	0.0984	–	–	–	–	0.00007	989.9	1000	940.7
7	0.96382	0.0448	0.0542	0.0387	–	–	–	–	0.00002	989.9	1000	940.7
8	0.95662	0.0057	0.0069	0.0049	–	–	–	–	0.00002	989.9	1000	940.7
T		5.26	5.21	5.30		2.82	2.80	2.84		4.07	4.06	4.11
λ		1	1.0371	0.9728		1	1.0144	0.9772		1	1.0025	0.9876
N_0			874				10 000				10^6	

to the data in Table 2. Since we want the process to have reached its quasi equilibrium distribution around $\boldsymbol{u}$ by the time of the first measurement, we require a burn in period. It has previously been shown that the equilibrium distribution is reached within a few generations (Jorde and Ryman, 1995; Waples and Yokota, 2007). This agrees with our experience and we consider the first 20 time steps as a burn in time for all three species. In every simulation, the species is initiated at time -20 with allele frequencies in each age class equal to 0.5, i.e. $\boldsymbol{Z}_{-20} = \boldsymbol{Y}_{-20} = 0.5N_{-20}\boldsymbol{u}$ rounded to the closest integer. In order to have the same total population size at time 0, we normalize the number of individuals in all age classes by multiplying $\boldsymbol{N}_0$ with a constant γ so that N_0 equals the corresponding pre-specified value in Table 2. Since we want γ to be as close to 1 as possible, we let $N_{-20} = \lambda^{-20}N_0$.

Beginning at time step 0, we calculate the allele frequency at every time step in two ways, by weighting the age classes with the vector $\boldsymbol{v}$ and with the vector $\mathbf{1}$. From time step 1 we estimate the standardized allele frequency variance for every time step using a modified version of the estimate presented by Nei and Tajima (1981). We measure all individuals and estimate the standardized allele frequency change variance $F^{\boldsymbol{c}}(\tau) = E((p^{\boldsymbol{c}}_{t+\tau} - p^{\boldsymbol{c}}_t)^2 | N^{\boldsymbol{c}}_t, p^{\boldsymbol{c}}_t)/(p^{\boldsymbol{c}}_t(1-p^{\boldsymbol{c}}_t))$ with

$$\hat{F}^{\boldsymbol{c}}(\tau) = \frac{\sum_{i=1}^{a}(p^{\boldsymbol{c}}_0(i) - p^{\boldsymbol{c}}_\tau(i))^2}{\sum_{i=1}^{a} p^{\boldsymbol{c}}_0(i)(1-p^{\boldsymbol{c}}_0(i))}, \tag{18}$$

where i is the order number of each simulation and a is the number of repeated simulations. The estimate $\hat{F}^{\boldsymbol{c}}(\tau)$ in (18) is a weighted average of the standardized allele frequency change variance for all repeated simulations. In this way, repetitions with allele frequencies close to 0.5 are given highest weight, similarly as in Jorde and Ryman (2007). To estimate the variance population size we use

$$\hat{N}^{\boldsymbol{c}}_{eV,t}(\tau) = \frac{\tau}{T\hat{F}^{\boldsymbol{c}}(\tau)}. \tag{19}$$

We assume that the whole population is measured at time points 0 and τ. Therefore, (19) is an estimator of (15) based on Monte Carlo approximations of the allele frequency change.

The results of the simulations, and comparisons with calculated values for the variance effective population size according to (15), are shown in Fig. 1. Although we use a large population assumption, we see that the values calculated from (15) are close to the simulated ones, calculated from (19) in all figures except for the growing scenario for barnacles, where the simulated values differ from the calculated ones when τ is large. However, repeated simulations with more samples resulted in a better fit. Hence the discrepancy is mainly due to random effects in the simulations. In all cases we also notice that when τ is large the weighting scheme becomes less important.

In order to validate our approximations when the reproductive variances differ from the Poisson model, we performed a simulation with the parameters from the stable scenario for sparrows in Table 2. To obtain a different variance structure, we let the number of offspring for breeding individuals be distributed according to a negative binomial distribution with mean b_i and variance $b_i + \beta$, where β varies from 0.1 to 50, and estimate N_{eV} when $\tau = 1$. The result of the simulation is shown in Fig. 2. As expected, N_{eV} decreases when the offspring distribution variance increases, and the simulated values agree with those calculated from (9).

6. Asymptotics of the variance effective population size

In the previous section we saw that the variance effective population size calculated with reproductive values as weights, for large τ seems to predict the asymptotic values of N_{eV} calculated with uniform weights. The same pattern appeared in the simulations by Jorde and Ryman (1995) and Waples and Yokota (2007). Increased time between measurements in the temporal method was one of their proposals to minimize the influence of the initial fluctuations due to the age structure when estimating N_{eV}.

In this section, we study how N_{eV} for a general scheme of weights behaves asymptotically as τ becomes large. Since we do not allow for new mutations in our model we assume a quasi equilibrium (Darroch and Seneta, 1965; Hössjer and Ryman, 2013; Collet et al., 2013), that is, we condition on that no allele gets fixed in the population. This conditioning corresponds to assumptions that underlie a multilocus estimate of N_{eV} based on allele frequency change from a number of markers, whose alleles have not yet been fixed.

Let

$$\Delta_{\boldsymbol{c}}(\tau) = \frac{N^{\boldsymbol{c}}_{eV,t}(\tau) - N^{\boldsymbol{v}}_{eV,t}(\tau)}{N^{\boldsymbol{v}}_{eV,t}(\tau)}, \tag{20}$$

be the relative discrepancy of $N^{\boldsymbol{c}}_{eV,t}(\tau)$ compared to $N^{\boldsymbol{v}}_{eV,t}(\tau)$. It turns out that the limit of the relative discrepancy for large τ depends on the growth rate and three cases, $\lambda = 1$, $\lambda > 1$ and $\lambda < 1$, have to be analyzed separately.

In Appendix G we show that when $\lambda = 1$, i.e. when the population size is expected to be stable, the relative discrepancy

$$\Delta_{\boldsymbol{c}}(\tau) \approx \frac{C}{\tau}, \tag{21}$$

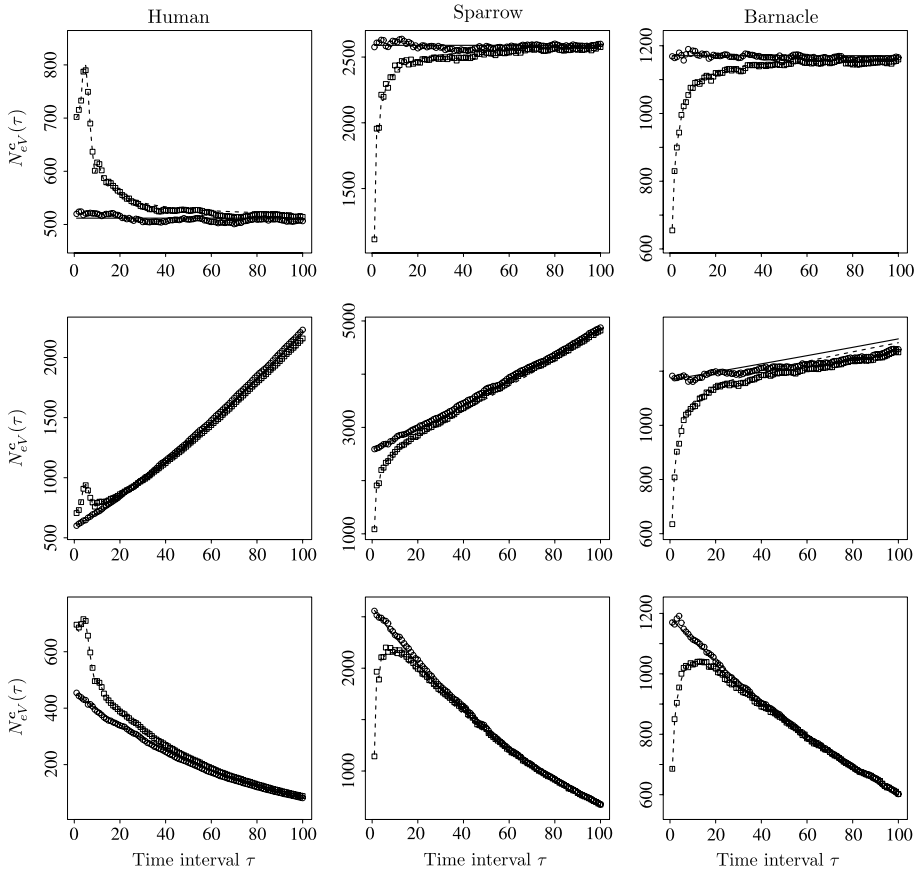

Fig. 1. Plots of simulated and analytically derived values of the variance effective population size for the human data (left), sparrow data (center) and barnacle data (right), for the stable scenario (top), growing scenario (middle), and decreasing scenario (bottom). Circles and squares represent values of the variance effective population size based on simulations (Eq. (19)) when $\boldsymbol{c} = \boldsymbol{v}$ and $\boldsymbol{c} = \mathbf{1}$, respectively. The solid line is the variance effective population size (Eq. (16)) calculated with the parameters in Table 2 with $\boldsymbol{c} = \boldsymbol{v}$ and the dashed line the corresponding effective population size when $\boldsymbol{c} = \mathbf{1}$. On the x-axis, time is measured in 5 year periods for humans, 1 year periods for sparrows and barnacles, and the first sample was taken at time point 0. Note the varying scale on the y-axis.

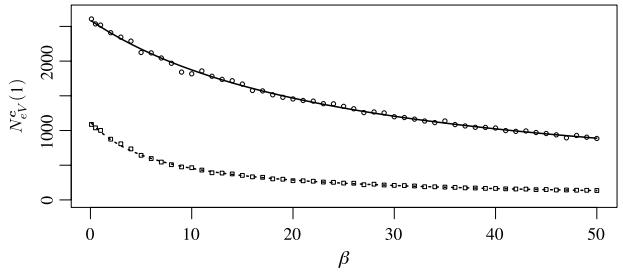

Fig. 2. Plot of simulated and analytically derived values of the variance effective population size for the stable sparrows data from Table 2 when the variance of offspring per individual varies. The effective population size is calculated at time point 1 where circles and squares represent the effective population size based on simulations (Eq. (19)) when $\boldsymbol{c} = \boldsymbol{v}$ and $\boldsymbol{c} = \mathbf{1}$ respectively. The solid (dashed) line is the variance effective population size (Eq. (16)) calculated with the parameters in Table 2 when $\boldsymbol{c} = \boldsymbol{v}$ ($\boldsymbol{c} = \mathbf{1}$). The number of offspring for the breeding age classes are distributed according to a negative binomial distribution with mean b_i and variance $b_i + \beta$.

where C is a constant derived in Appendix G. Hence, the relative discrepancy for any weight vector, compared to $\boldsymbol{v}$, can be made arbitrarily small by increasing the number of time steps between the two measurements in the temporal method. In particular, this means that using reproductive values as weights when calculating N_{eV} will accurately predict the asymptotic value of N_{eV} calculated with uniform weights. In Fig. 3, $\tau\Delta_{\boldsymbol{c}}(\tau)$, the relative discrepancy, scaled by τ, and $\Delta_{\boldsymbol{c}}(\tau)$, are plotted for the stable scenarios of the species in Table 2. The relative discrepancy scaled by τ illustrates at which rate the discrepancy declines and we see that it converges to the asymptotic limit C. We also see that the relative discrepancy converges to zero as expected.

Table 3
Time, in generations, for human, sparrow and barnacle life tables needed to obtain a relative discrepancy (Eq. (20)) of α for $\boldsymbol{c} = \mathbf{1}$. A positive direction of bias indicates overestimation, and a negative direction indicates underestimation of N_{eV}.

Species	NoGen			Direction of bias
	$\alpha = 0.1$	$\alpha = 0.05$	$\alpha = 0.01$	
Human	3.04	6.08	30.4	Positive
Sparrow	3.14	6.28	31.4	Negative
Barnacle	2.18	4.36	21.8	Negative

The constant C can be used to calculate a minimal time interval required for a certain level of tolerated relative discrepancy. For instance, if a relative discrepancy (Eq. (21)) of α is tolerated, the number of generations between measurements (NoGen) must satisfy

$$\text{NoGen} \geq \frac{C}{\alpha T}.$$

In Table 3, we see that the time, in generations, needed between measurements for different values of α differs between humans, sparrows and barnacles. It also shows that N_{eV} can be both over- and underestimated when a uniform weighting scheme is used.

When the population size is expected to grow, i.e. $\lambda > 1$, the relative discrepancy converges to a constant as τ becomes large. For populations with $\lambda < 1$, we have to assume a large initial population so that the population survives a large number of time steps, then the relative discrepancy tends to a constant as τ grows.

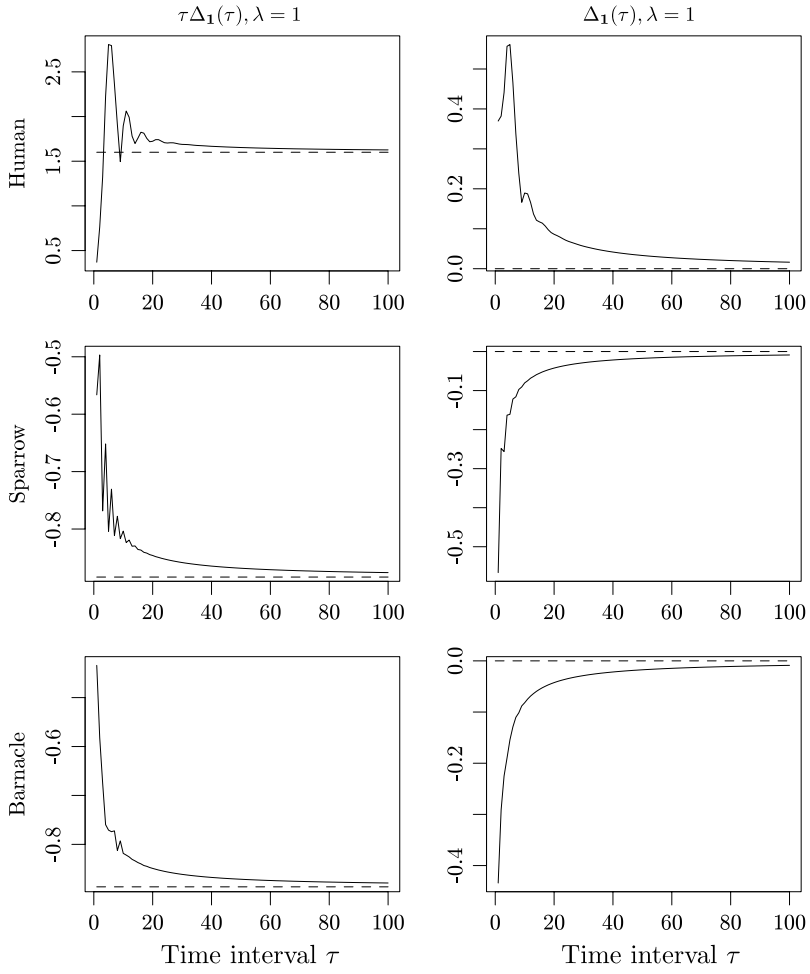

Fig. 3. Plots of the scaled relative discrepancy (left) and the relative discrepancy (right) (Eq. (20)), represented by the solid lines, for the stable scenario for the species in Table 2. The dashed lines are the asymptotic limits (Eq. (G.3)) which are zero for the right columns. On the *x*-axis, time is measured in 5 year periods for humans, 1 year periods for sparrows and barnacles.

Both constants are derived in Appendix G. For both growing and decreasing populations the relative discrepancy will be close to zero when λ is close to one. In Fig. 4, the relative discrepancy is plotted for the growing and decreasing scenarios for the species in Table 2.

In Fig. 5, we have calculated the asymptotic limit of the relative discrepancy $\Delta_1(\tau)$, as τ becomes large, as a function of the growth rate. The parameters b_i and σ_i for the stable scenario for sparrows in Table 2 have been multiplied by constants ranging from 0.2 to 4 in order to vary λ. For growth rates less than one, the relative discrepancy is close to zero, but for populations with growth rate greater than one, the magnitude of the discrepancy grows when λ becomes larger. Although these calculations are based on a single species' demographic parameters, it is an indication that, for species with $\lambda > 1$, weighting individuals according to their age classes' reproductive values does not always result in a good prediction of the asymptotic value of N_{eV}, calculated with uniform weights.

7. Discussion

In this paper we have extended previous approaches to derive explicit approximations of N_{eV} for two points in time separated by arbitrary intervals, with a special focus on models for age-structured populations of non-constant size. Previous expressions for N_{eV} have focused on the allele frequency change of the whole population when age classes are weighted by their reproductive values. However, uniform weights give the actual allele frequency of the population and are therefore in some sense the most natural to study. We have investigated when N_{eV} for uniform weights based on allele frequency changes over long time periods, can be well approximated by N_{eV} for reproductive weights based on allele frequency changes over shorter time periods.

Our approach is similar to that of Nagylaki (1980) and Hössjer and Ryman (2013), who studied allele frequency fluctuations in time for sub-structured populations in which the subpopulation sizes are constant, and migration more or less strong. Hössjer and Ryman (2013) derived explicit approximations of N_{eV} for two consecutive points in time, and our current work represents an extension to arbitrary time intervals of measurements for models in which subpopulation sizes are allowed to fluctuate in time, and these subpopulations represent age classes. However, these stochastic fluctuations of age class sizes are relatively modest in our model and they will have a minor impact on N_{eV}, unless the population is small.

We demonstrated that the allele frequency change can be decomposed into a sum of two terms, of which the first reflects the genetic drift of the whole population. This term has previously been included in N_{eV} calculations (Engen et al., 2005a). The second, novel, term depends on allele frequency fluctuations between age classes around a stable fix point, obtained as the leading right eigenvector of the expected projection or Leslie matrix of birth and survival rates, and it only vanishes when reproductive weights are used. For other schemes, the relative importance of these two sources of allele frequency change will depend on the

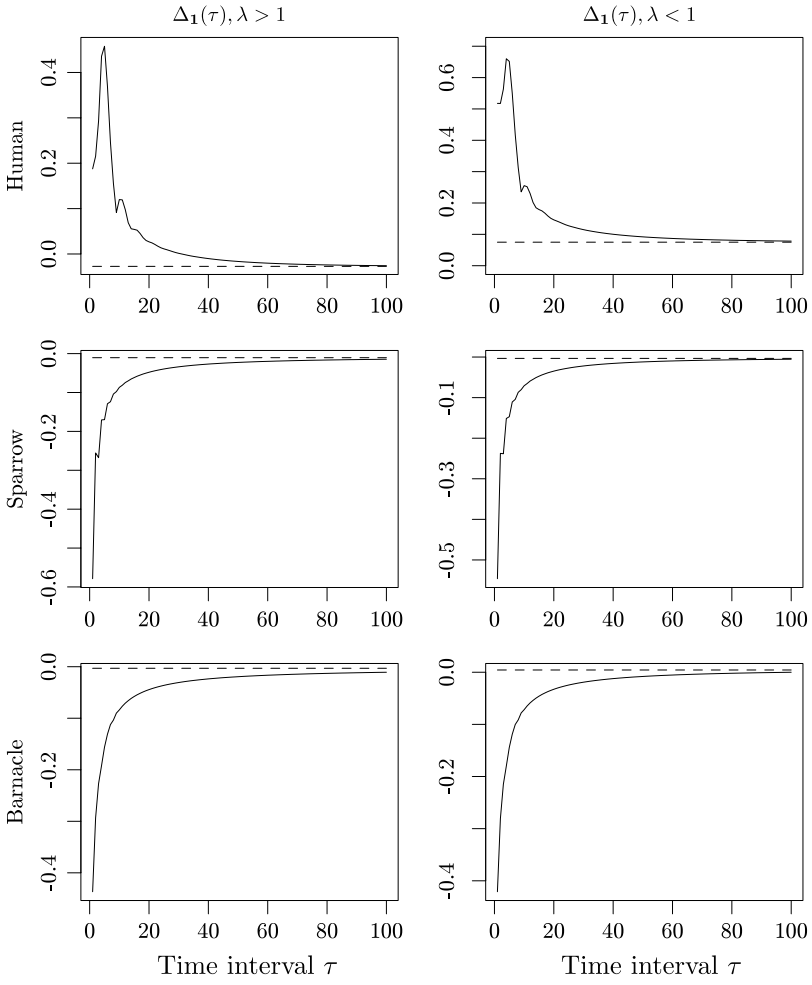

Fig. 4. Plots of the relative discrepancy (Eq. (20)) for the growing scenario (left) and the decreasing scenario (right), represented by the solid lines, for the species in Table 2, when weights $\boldsymbol{c} = \mathbf{1}$ are used. The dashed lines are the asymptotic limits (Eqs. (G.4) and (G.5)) which are, for the growing (decreasing) scenario, −0.0273 (0.0750) for humans, −0.0105 (−0.0034) for sparrows and −0.0030 (0.0043) for barnacles. On the *x*-axis, time is measured in 5 year periods for humans, 1 year periods for sparrows and barnacles.

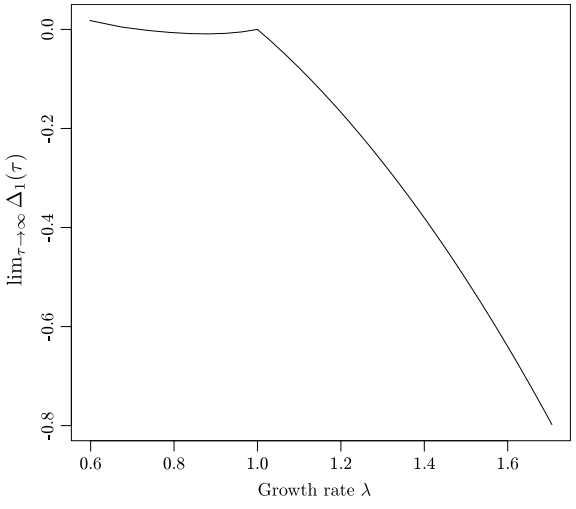

Fig. 5. The asymptotic limit (Eqs. (G.3)–(G.5)) as $\tau \to \infty$ for the relative discrepancy of $N_{eV}^{1}(\tau)$, compared to $N_{eV}^{\mathbf{v}}(\tau)$, plotted as a function of λ, for the sparrows data from Table 2. The growth rate λ has been varied by multiplying b_i and σ_i for the stable scenario by constants ranging from 0.2 to 4.

average growth rate of the population as well as the time between measurements. This delicate balance between the two sources of allele frequency change has several implications. First, the allele frequency change over long time intervals will not depend on the weighting scheme when the expected population size is constant, and in particular the reproductive and uniform weights will give the same result. The reason is that the second novel term will have a negligible impact on the allele frequency change over long time intervals, whereas the first dominating term will largely be independent of the weighting scheme. Therefore, the actual variance in allele frequency change over longer time periods is accurately predicted by N_{eV} using any kind of weighting scheme.

Second, for populations in which the expected population size grows or declines, the long term expression for the variance effective size will depend on the weighting scheme. Third, the variance effective size will exhibit initial transient fluctuations as a function of the time between measurements. These initial fluctuations are generally of no interest for age-structured models. However, for spatial and other types of structured models, with a slower migration rate, they describe the short term transient behavior of N_{eV}. Fourth, for reproductive weights, the long term genetic drift can be predicted from the short term genetic drift over one single time step, provided the expected population size is constant, since the above mentioned initial fluctuations are essentially canceled out. Finally, for other population growth scenarios, we present a formula for the relative discrepancy between the long term N_{eV} based on reproductive and uniform (or some other) weighting

scheme. It turns out that for populations with a close to constant expected size, this discrepancy will be small. Using reproductive weights will then give a good approximation of the genetic drift and N_{eV}.

Theoretical characterization of N_{eV} such as our current work is important for analyzing how various assumptions impact the variance effective population size. For instance, our results enable studies on how different demographic parameters affect N_{eV}, and this makes it possible to study how demographic manipulation affects N_{eV}, for instance how harvest strategies focused on separate age classes influence N_{eV}. Such analyses are of high relevance for fisheries, wildlife and conservation management (Ryman et al., 1981; Allendorf et al., 2008; Sæther et al., 2009). Hence, development of new formulas allowing relaxation from ideal conditions is important in order to increase our understanding of the mechanisms of N_{eV}.

Our findings show that the estimate by the temporal method strongly depends on how the age classes are weighted together when estimating the allele frequency change. In case that life tables (i.e. age-specific birth and survival rates) are not known, and the population size is constant in time, the long term genetic drift can be estimated by increasing the time span between the measurements, as proposed by Jorde and Ryman (1995) and Waples and Yokota (2007). On the other hand, if life tables are known, unbiased estimates of the long term genetic drift can be obtained over short time spans by using the reproductive weights, since this will approximate the long term genetic drift well in most cases. Other methods for calculating estimators of the long term N_{eV} using life tables have previously been presented by Jorde and Ryman (1995, 1996) and Jorde (2012). However, when the population size is expected to grow or decline, the discrepancy of N_{eV} for the different weighting schemes will increase.

With our method it is possible to explore for empirical situations how long time intervals are necessary between measurements to be able to ignore the effects of overlapping generations for various life tables. We see in Table 3 that the time needed between measurements for a specific level of relative discrepancy differs between the species, and that N_{eV} can be both over- and underestimated (cf. Jorde and Ryman, 1995; Waples and Yokota, 2007). Waples and Yokota (2007) suggested a minimum of three to five generations between the measurements in order to minimize the bias. However, it is clear from Table 3 that such a rule of thumb cannot be applied generally without considering the magnitude of acceptable bias and the demographic characteristics of the population under study.

When analyzing the temporal method analytically and by simulations in the present study, we have, for simplicity, assumed that all individuals in all age classes of the population are measured at both points in time. In empirical situations when only a fraction of the population can be measured, one needs to adjust for the additional sampling variation in order to reduce the bias of the estimated variance effective population size. We intend to address this issue in a follow-up paper, generalizing the estimation method of Jorde and Ryman (2007) for demographically homogeneous populations to models with age-structure.

Acknowledgments

Financial support from the Swedish Research Council, contract nr. 621-2008-4946, and the Gustafsson Foundation for Research in Natural Sciences and Medicine to Ola Hössjer is acknowledged, as is support from the Swedish Environmental Protection Agency and the Swedish Research Council Formas to Linda Laikre, and support to Nils Ryman from the Swedish Research Council and the Swedish Research Council Formas. We also wish to thank two anonymous reviewers for valuable comments.

Appendix A. Description of G_t, H_t, (10) and (11)

Each individual $k \in \{1, \dots, N_{ti}\}$ in generation t and age class i gives birth to B_{tik} progeny with $E(B_{tik}) = b_i$ and $\mathrm{Var}(B_{tik}) = \sigma_i^2$. Let I_{tik} be the indicator that individual k in age class i of generation t survives to age $i+1$ with $\rho_i = \mathrm{Corr}(I_{tik}, B_{tik})$ and $E(I_{tik}) = s_i$.

Assuming that individuals are numbered so that the first Z_{tj} have the specified allele, we find that the non-zero elements of the projection matrix $\boldsymbol{G}_t$ are given by

$$\begin{aligned} G_{t0j} &= Z_{tj}^{-1} \sum_{k=1}^{Z_{tj}} B_{tjk}, \\ G_{t,j+1,j} &= Z_{tj}^{-1} \sum_{k=1}^{Z_{tj}} I_{tjk}, \quad j = 0, \dots, n-2, \end{aligned} \tag{A.1}$$

and similarly the non-zero elements for $\boldsymbol{H}_t$

$$\begin{aligned} H_{t0j} &= Y_{tj}^{-1} \sum_{k=Z_{tj}+1}^{Z_{tj}+Y_{tj}} B_{tjk}, \\ H_{t,j+1,j} &= Y_{tj}^{-1} \sum_{k=Z_{tj}+1}^{Z_{tj}+Y_{tj}} I_{tjk}, \quad j = 0, \dots, n-2. \end{aligned} \tag{A.2}$$

To get an explicit expression for (10) we first notice that the column vector $\boldsymbol{\delta}_{tj} = \boldsymbol{G}_{tj} - g_j = (\delta_{t,ji})$ have two non-zero elements $\delta_{tj0} = G_{t0j} - b_j$ and $\delta_{t,j+1,j} = G_{t,j+1,j} - s_j$. Since

$$\boldsymbol{C}_j = Z_{tj}\,\mathrm{Cov}(\delta_{tj}) = (\boldsymbol{C}_{j,i_1 i_2})_{i_1,i_2=0}^{n-1}$$

we see that (10) has non-zero elements

$$\begin{aligned} C_{j00} &= Z_{tj}\mathrm{Var}(G_{t0j} - b_j) \\ &= Z_{tj}\mathrm{Var}\left(Z_{tj}^{-1}\sum_{k=1}^{Z_{tj}} B_{tjk}\right) \\ &= \mathrm{Var}(B_{tjk}) \\ &= \sigma_j^2, \\ C_{j,j+1,j+1} &= s_j(1-s_j), \\ C_{j,0,j+1} &= C_{j,j+1,0} = \sigma_j\sqrt{s_j(1-s_j)}\rho_j. \end{aligned}$$

Hence, $\boldsymbol{\Sigma} = (\Sigma_{ij})$ has non-zero elements along the diagonal and first row and column, given by

$$\begin{aligned} \Sigma_{00} &= \sum_{i=0}^{n-1} u_i\sigma_i^2, \\ \Sigma_{i+1,i+1} &= u_i s_i(1-s_i), \quad i = 0, \dots, n-2, \\ \Sigma_{0,i+1} &= \Sigma_{i+1,0} = u_i\sigma_i\sqrt{s_i(1-s_i)}\rho_i, \quad i = 0, \dots, n-2. \end{aligned} \tag{A.3}$$

□

Appendix B. Calculation of u, v and T

Although $\boldsymbol{u}$ and $\boldsymbol{v}$ can be derived as left and right eigenvectors of $\boldsymbol{g}$, following Engen et al. (2005a), it is also possible to derive more explicit formulas. The elements of the stable age distribution, $\boldsymbol{u}$, are given by

$$u_i = \frac{l_i\lambda^{-i-1}}{\sum_{j=0}^{n-1} l_j\lambda^{-j-1}}, \tag{B.1}$$

where $l_i = \prod_{j=0}^{i-1} s_j$ is the probability that an individual survives to age class i. The elements of the vector of reproductive values, $\boldsymbol{v}$, are given by

$$v_i \propto \frac{\lambda^i}{l_i}\sum_{j=i}^{n-1} l_j b_j \lambda^{-j-1}, \tag{B.2}$$

where $\propto$ denotes proportionality. The vector $\boldsymbol{v}$ is normalized so that $\boldsymbol{vu} = 1$ holds. The generation time T is given by

$$T = \sum_{i=0}^{n-1}(i+1)l_i b_i \lambda^{-i-1}. \quad \square$$

Appendix C. Verifying (7) and (14)

By rewriting the difference in allele frequencies between time t and $t+\tau$ we have that

$$\begin{aligned} p^{\boldsymbol{c}}_{t+\tau} - p^{\boldsymbol{c}}_t &= \frac{Z^{\boldsymbol{c}}_{t+\tau}}{Z^{\boldsymbol{c}}_{t+\tau} + Y^{\boldsymbol{c}}_{t+\tau}} - \frac{\lambda^\tau Z^{\boldsymbol{c}}_t}{\lambda^\tau (Z^{\boldsymbol{c}}_t + Y^{\boldsymbol{c}}_t)} \\ &\approx \frac{1}{\lambda^\tau (Z^{\boldsymbol{c}}_t + Y^{\boldsymbol{c}}_t)}(Z^{\boldsymbol{c}}_{t+\tau} - \lambda^\tau Z^{\boldsymbol{c}}_t) \\ &\quad - \frac{Z^{\boldsymbol{c}}_t}{\lambda^\tau (Z^{\boldsymbol{c}}_t + Y^{\boldsymbol{c}}_t)^2}(Z^{\boldsymbol{c}}_{t+\tau} - \lambda^\tau Z^{\boldsymbol{c}}_t + Y^{\boldsymbol{c}}_{t+\tau} - \lambda^\tau Y^{\boldsymbol{c}}_t) \\ &= \frac{1-p^{\boldsymbol{c}}_t}{\lambda^\tau N^{\boldsymbol{c}}_t}(Z^{\boldsymbol{c}}_{t+\tau} - \lambda^\tau Z^{\boldsymbol{c}}_t) - \frac{p^{\boldsymbol{c}}_t}{\lambda^\tau N^{\boldsymbol{c}}_t}(Y^{\boldsymbol{c}}_{t+\tau} - \lambda^\tau Y^{\boldsymbol{c}}_t), \end{aligned}$$

where in the second step we made a first order Taylor expansion, valid for large populations. We define the demographic variance

$$\sigma^2_{d,\boldsymbol{c}}(\tau) = \frac{1}{\lambda^{2\tau} Z^{\boldsymbol{c}}_t} E\left((Z^{\boldsymbol{c}}_{t+\tau} - \lambda^\tau Z^{\boldsymbol{c}}_t)^2 | Z^{\boldsymbol{c}}_t\right), \tag{C.1}$$

which is similar to the definition in Engen et al. (2005b). We assume that the right hand side of (C.1) is independent of $Z^{\boldsymbol{c}}_t$, which is a good approximation for large populations. Therefore, it follows from (C.1) and symmetry of segregation of both alleles that

$$\begin{aligned} \sigma^2_{d,\boldsymbol{c}}(\tau) &= \frac{1}{\lambda^{2\tau} Z^{\boldsymbol{c}}_t} E\left((Z^{\boldsymbol{c}}_{t+\tau} - \lambda^\tau Z^{\boldsymbol{c}}_t)^2 | Z^{\boldsymbol{c}}_t\right) \\ &= \frac{1}{\lambda^{2\tau} Y^{\boldsymbol{c}}_t} E\left((Y^{\boldsymbol{c}}_{t+\tau} - \lambda^\tau Y^{\boldsymbol{c}}_t)^2 | Y^{\boldsymbol{c}}_t\right). \end{aligned}$$

Consequently, the expected allele frequency change from time t to $t+\tau$ can be calculated as

$$\begin{aligned} E((p^{\boldsymbol{c}}_{t+\tau} - p^{\boldsymbol{c}}_t)^2 | N^{\boldsymbol{c}}_t, p^{\boldsymbol{c}}_t) &= E((p^{\boldsymbol{c}}_{t+\tau} - p^{\boldsymbol{c}}_t)^2 | Z^{\boldsymbol{c}}_t, Y^{\boldsymbol{c}}_t) \\ &\approx \frac{(1-p^{\boldsymbol{c}}_t)^2}{\lambda^{2\tau}(N^{\boldsymbol{c}}_t)^2} E((Z^{\boldsymbol{c}}_{t+\tau} - \lambda^\tau Z^{\boldsymbol{c}}_t)^2 | Z^{\boldsymbol{c}}_t) \\ &\quad + \frac{(p^{\boldsymbol{c}}_t)^2}{\lambda^{2\tau}(N^{\boldsymbol{c}}_t)^2} E((Y^{\boldsymbol{c}}_{t+\tau} - \lambda^\tau Y^{\boldsymbol{c}}_t)^2 | Y^{\boldsymbol{c}}_t) \\ &= \frac{1}{\lambda^{2\tau}(N^{\boldsymbol{c}}_t)^2}((1-p^{\boldsymbol{c}}_t)^2 \lambda^{2\tau} \sigma^2_{d,\boldsymbol{c}}(\tau) Z^{\boldsymbol{c}}_t \\ &\quad + (p^{\boldsymbol{c}}_t)^2 \lambda^{2\tau} \sigma^2_{d,\boldsymbol{c}}(\tau) Y^{\boldsymbol{c}}_t) \\ &= \frac{\sigma^2_{d,\boldsymbol{c}}(\tau)}{N^{\boldsymbol{c}}_t}((1-p^{\boldsymbol{c}}_t)^2 p^{\boldsymbol{c}}_t + (1-p^{\boldsymbol{c}}_t)(p^{\boldsymbol{c}}_t)^2) \\ &= \frac{p^{\boldsymbol{c}}_t (1-p^{\boldsymbol{c}}_t)\sigma^2_{d,\boldsymbol{c}}(\tau)}{N^{\boldsymbol{c}}_t}, \end{aligned} \tag{C.2}$$

in accordance with (14). In the second step of (C.2) we assumed that the two alleles segregate independently, so that the covariance term vanishes. The reason is that we have a haploid population in which individuals produce offspring independently of each other. To verify (7) we let $\tau = 1$ and proceed as above. $\square$

Appendix D. Verifying (12) and (13)

Let $\lambda_0\ (=\lambda), \lambda_1, \ldots, \lambda_{n-1}$ be the (possibly complex valued) eigenvalues of $\boldsymbol{g}$, listed in descending order with respect to their moduli, and let $\boldsymbol{g} = \boldsymbol{Q\Lambda Q}^{-1}$ be its Jordan canonical form. The matrix $\boldsymbol{\Lambda}$ is upper triangular (see for instance Grimmett and Stirzaker, 2001) with $\lambda_0, \ldots, \lambda_{n-1}$ along the diagonal, so that $\boldsymbol{u}$ is the first column of $\boldsymbol{Q}$ and $\boldsymbol{v}$ the first row of $\boldsymbol{Q}^{-1}$. In particular, when all λ_i are distinct, $\boldsymbol{\Lambda}$ is diagonal, all columns of $\boldsymbol{Q}$ are right eigenvectors of $\boldsymbol{g}$ and all rows of $\boldsymbol{Q}^{-1}$ left eigenvectors of $\boldsymbol{g}$. Let $Z_t = Z^{\boldsymbol{v}}_t = \boldsymbol{vZ}_t$, $Y_t = Y^{\boldsymbol{v}}_t = \boldsymbol{vY}_t$ and put

$$\boldsymbol{Z}_t = \boldsymbol{\Pi}_1 \boldsymbol{Z}_t + \boldsymbol{\Pi}_2 \boldsymbol{Z}_t = Z_t \boldsymbol{u} + \epsilon_t, \tag{D.1}$$

where ϵ_t represents random fluctuations of $\boldsymbol{Z}_t$ around a vector proportional to $\boldsymbol{u}$. Similarly, write

$$\boldsymbol{Y}_t = \boldsymbol{\Pi}_1 \boldsymbol{Y}_t + \boldsymbol{\Pi}_2 \boldsymbol{Y}_t = Y_t \boldsymbol{u} + \varepsilon_t,$$

for the vector corresponding to the non-specified allele. Here $\boldsymbol{\Pi}_1 = \boldsymbol{Q}\boldsymbol{I}_1\boldsymbol{Q}^{-1}$, with $\boldsymbol{I}_1 = \mathrm{diag}(1, 0, \ldots, 0)$, is the projection onto the one-dimensional subspace $\mathcal{U}_1$ of $\mathbb{R}^n$ spanned by $\boldsymbol{u}$, and $\boldsymbol{\Pi}_2 = \boldsymbol{Q}\boldsymbol{I}_2\boldsymbol{Q}^{-1}$, with $\boldsymbol{I}_2 = \mathrm{diag}(0, 1, \ldots, 1)$, is the projection onto the $n-1$-dimensional subspace $\mathcal{U}_2$ of $\mathbb{R}^n$ spanned by the remaining $n-1$ columns of $\boldsymbol{Q}$. Put also $\tilde{\boldsymbol{g}} = \boldsymbol{\Pi}_2 \boldsymbol{g} = \boldsymbol{Q}\tilde{\boldsymbol{\Lambda}}\boldsymbol{Q}^{-1}$, with $\tilde{\boldsymbol{\Lambda}} = \boldsymbol{I}_2\boldsymbol{\Lambda}$ for the projection of $\boldsymbol{g}$ onto $\mathcal{U}_2$.

In order to obtain an explicit expression for the demographic variance, we let

$$\boldsymbol{V}_t = \frac{E(\epsilon_t(\epsilon_t)' | Z_t)}{Z_t}.$$

We first observe that

$$\begin{aligned} \frac{E(\epsilon_{t+1}(\epsilon_{t+1})' | Z_t)}{Z_t} &= \frac{Z_{t+1}}{Z_t}\frac{E(\epsilon_{t+1}(\epsilon_{t+1})' | Z_t)}{Z_{t+1}} \\ &\approx \lambda \frac{E(\epsilon_{t+1}(\epsilon_{t+1})' | Z_{t+1})}{Z_{t+1}} \\ &= \lambda \boldsymbol{V}_{t+1}. \end{aligned} \tag{D.2}$$

The second step of (D.2) relies on a large population assumption, so that (4) is an accurate approximation, and moreover, the genetic drift is so small that changing conditioning from Z_t to Z_{t+1} has little effect on $E(\epsilon_{t+1}(\epsilon_{t+1})' | Z_t)$. Then, using (D.1) we see that

$$\begin{aligned} \epsilon_{t+1} &= \boldsymbol{\Pi}_2 \boldsymbol{Z}_{t+1} \\ &= \boldsymbol{\Pi}_2(\boldsymbol{g}\boldsymbol{Z}_t + \boldsymbol{\delta}_t \boldsymbol{Z}_t) \\ &= \boldsymbol{\Pi}_2 \boldsymbol{g}\boldsymbol{Z}_t + \boldsymbol{\Pi}_2 \sum_{i=0}^{n-1} \boldsymbol{\delta}_{ti} Z_{ti} \\ &\approx \boldsymbol{g}\epsilon_t + \boldsymbol{\Pi}_2 Z_t \sum_{i=0}^{n-1} \boldsymbol{\delta}_{ti} u_i. \end{aligned}$$

Hence,

$$\begin{aligned} \frac{E(\epsilon_{t+1}(\epsilon_{t+1})' | Z_t)}{Z_t} &\approx \boldsymbol{g}\boldsymbol{V}_t\boldsymbol{g}' + \sum_{i=0}^{n-1} \boldsymbol{\Pi}_2 \boldsymbol{C}_i (\boldsymbol{\Pi}_2)' u_i \\ &= \boldsymbol{g}\boldsymbol{V}_t\boldsymbol{g}' + \boldsymbol{\Pi}_2 \boldsymbol{\Sigma} (\boldsymbol{\Pi}_2)', \end{aligned} \tag{D.3}$$

where we used $E(\boldsymbol{\delta}_t | \epsilon_t) = \boldsymbol{0}$, (10) and (11). Combining (D.2) and (D.3) we get a recursion formula

$$\boldsymbol{V}_{t+1} = \lambda^{-1}\boldsymbol{g}\boldsymbol{V}_t(\boldsymbol{g})' + \lambda^{-1}\boldsymbol{\Pi}_2\boldsymbol{\Sigma}(\boldsymbol{\Pi}_2)',$$

for $\boldsymbol{V}_t$, which converges to

$$\begin{aligned} \boldsymbol{V} &= \sum_{k=0}^{\infty} \lambda^{-(k+1)} \boldsymbol{\Pi}_2 \boldsymbol{g}^k \boldsymbol{\Sigma} (\boldsymbol{g}^k)' \boldsymbol{\Pi}_2' \\ &= \lambda^{-1}\boldsymbol{\Pi}_2\boldsymbol{\Sigma}(\boldsymbol{\Pi}_2)' + \sum_{k=1}^{\infty} \lambda^{-(k+1)} \tilde{\boldsymbol{g}}^k \boldsymbol{\Sigma} (\tilde{\boldsymbol{g}}^k)', \end{aligned} \tag{D.4}$$

as $t \to \infty$, provided $|\lambda_1|^2/\lambda < 1$, since $|\lambda_1|$ is the largest modulus of the eigenvalues of $\tilde{\boldsymbol{g}}$. Hence, we have motivated that

$$\boldsymbol{V}_t \approx \boldsymbol{V}. \tag{D.5}$$

We then use (D.1) to see that

$$Z^{\boldsymbol{c}}_{t+\tau} - \lambda^\tau Z^{\boldsymbol{c}}_t = \boldsymbol{c}\prod_{s=0}^{\tau-1}(\boldsymbol{g}+\boldsymbol{\delta}_{t+s})(Z_t\boldsymbol{u}+\epsilon_t) - \lambda^\tau \boldsymbol{c}(Z_t\boldsymbol{u}+\epsilon_t)$$
$$\approx \boldsymbol{c}Z_t\sum_{s=0}^{\tau-1}\lambda^s\boldsymbol{g}^{\tau-s-1}\boldsymbol{\delta}_{t+s}\boldsymbol{u} + \boldsymbol{c}(\boldsymbol{g}^\tau - \lambda^\tau\boldsymbol{I})\epsilon_t. \qquad (D.6)$$

The first term on the right hand side of (D.6) reflects genetic drift $(\boldsymbol{\delta}_t, \ldots, \boldsymbol{\delta}_{t+\tau})$ over τ time steps and the second term random demographic variation of allele frequencies between age classes (ϵ_t). In view of (11), the first half of (13), (D.5), and an approximation for large populations, whereby we can replace Z^c_t by Z_t, it follows that the demographic variance can be approximated by

$$\sigma^2_{d,\boldsymbol{c}}(\tau) \approx \frac{1}{\lambda^{2\tau}Z_t}E\left((Z^c_{t+\tau} - \lambda^\tau Z^c_t)^2|Z_t\right)$$
$$= \lambda^{-\tau-1}\boldsymbol{c}\left(\sum_{r=0}^{\tau-1}\lambda^{-r}\boldsymbol{g}^r\boldsymbol{\Sigma}(\boldsymbol{g}^r)'\right)\boldsymbol{c}'$$
$$+\lambda^{-2\tau}\boldsymbol{c}(\boldsymbol{g}^\tau - \lambda^\tau\boldsymbol{I})\boldsymbol{V}(\boldsymbol{g}^\tau - \lambda^\tau\boldsymbol{I})'\boldsymbol{c}'.$$

To verify (12) we let $\tau = 1$ and proceed as above. □

Appendix E. Using $\boldsymbol{c} = \boldsymbol{v}$ in (12)

The demographic variance presented in Engen et al. (2005a) is the same expression when we let $\boldsymbol{c} = \boldsymbol{v}$ in (12). In order to show this, we first let $\boldsymbol{v}^E = (v^E_0, \ldots, v^E_{n-1})$ be the reproductive values used in Engen et al. (2005a) which are proportional to v_i and equal to the right hand side of (B.2), and therefore normalized so that $v^E_0 = 1$ instead of (2). Then, we rewrite the expression for the demographic variance in Engen et al. (2005a) as

$$\sigma^2_d = \lambda^{-2}\sum_{i=0}^{n-1}u_i\left(\left(\frac{\partial\lambda}{\partial b_i}\frac{1}{u_i}\right)^2\sigma^2_i + \left(\frac{\partial\lambda}{\partial s_i}\frac{1}{u_i}\right)^2 s_i(1-s_i)\right.$$
$$\left.+2\frac{\partial\lambda}{\partial b_i}\frac{1}{u_i}\frac{\partial\lambda}{\partial s_i}\frac{1}{u_i}c_i\right)$$
$$= \lambda^{-2}\left(v_0^2\sum_{i=0}^{n-1}u_i\sigma^2_i + \sum_{i=0}^{n-2}u_is_i(1-s_i)v^2_{i+1}\right.$$
$$\left.+\sum_{i=0}^{n-2}v_0v_{i+1}2u_i\sigma_i\sqrt{s_i(1-s_i)}\rho_i\right)$$
$$= \lambda^{-2}\boldsymbol{v}\boldsymbol{\Sigma}\boldsymbol{v}',$$

where in the last step we employed formula (A.3) for the nonzero elements of $\boldsymbol{\Sigma}$ and in the second step we used (B.1), (B.2) and the fact that

$$\frac{\partial\lambda}{\partial b_i}\frac{1}{u_i} = \frac{l_i\lambda^{-i}}{T}\frac{\sum_{j=0}^{n-1}l_j\lambda^{-j-1}}{l_i\lambda^{-i-1}}$$
$$= \frac{\lambda v^E_0\sum_{j=0}^{n-1}l_j\lambda^{-j-1}}{T} = v_0,$$
$$\frac{\partial\lambda}{\partial s_i}\frac{1}{u_i} = \frac{l_i\lambda^{-i}v^E_{i+1}}{T}\frac{\sum_{j=0}^{n-1}l_j\lambda^{-j-1}}{l_i\lambda^{-i-1}}$$
$$= \frac{\lambda v^E_{i+1}\sum_{j=0}^{n-1}l_j\lambda^{-j-1}}{T} = v_{i+1}.$$

In the last step we used that $v_i = v^E_i\lambda\sum_{j=0}^{n-1}l_j\lambda^{-j-1}/T$, which follows from (2), the formula for v^E_i on the right hand side of (B.2) and the fact that $\sum_{i=0}^{n-1}u_iv^E_i = T/(\lambda\sum_{j=0}^{n-1}l_j\lambda^{-j-1})$. □

Appendix F. Explicit expression for $\boldsymbol{V}$

When $\boldsymbol{\Lambda}$ is diagonal, then $\tilde{\boldsymbol{g}}^k = \boldsymbol{Q}\tilde{\boldsymbol{\Lambda}}^k\boldsymbol{Q}^{-1}$ and $\tilde{\boldsymbol{\Lambda}}^k = \mathrm{diag}(0, \lambda^k_1, \ldots, \lambda^k_{n-1})$ for $k = 1, 2, 3, \ldots$, and hence the expression (D.4) for $\boldsymbol{V}$ can be written as

$$\boldsymbol{V} = \boldsymbol{Q}(\boldsymbol{A}\odot(\boldsymbol{Q}^{-1}\boldsymbol{\Sigma}(\boldsymbol{Q}^{-1})'))\boldsymbol{Q}',$$

where $\odot$ denotes elementwise multiplication and the elements of $\boldsymbol{A} = (A_{ij})$ are given by

$$A_{ij} = \lambda^{-1}1_{\{\min(i,j)\geq 1\}}\sum_{k=0}^{\infty}\frac{\lambda^k_i\lambda^k_j}{\lambda^k}$$
$$= \frac{\lambda^{-1}1_{\{\min(i,j)\geq 1\}}}{1-\frac{\lambda_i\lambda_j}{\lambda}}. \quad \square$$

Appendix G. Asymptotics of the variance effective population size

We will make use of the approximation in the second step of (15), and additionally assume that $N^{\boldsymbol{c}}_t \approx N^{\boldsymbol{v}}_t$, which, in view of (3) and the fact that $\boldsymbol{cu} = \boldsymbol{vu} = 1$, is accurate for large populations. By inserting (14) into (15) it then follows that the demographic variance appears in the denominator of $N^{\boldsymbol{c}}_{eV}(\tau)$ and it is the only quantity in this equation that depends on the weighting scheme $\boldsymbol{c}$. Hence, in view of the two above mentioned approximations, we can rewrite the relative discrepancy for $N^{\boldsymbol{c}}_{eV,t}(\tau)$ as

$$\Delta_{\boldsymbol{c}}(\tau) = \frac{-\tilde{\Delta}_{\boldsymbol{c}}(\tau)}{1+\tilde{\Delta}_{\boldsymbol{c}}(\tau)},$$

where

$$\tilde{\Delta}_{\boldsymbol{c}}(\tau) = \frac{\sigma^{\boldsymbol{c}}_d(\tau) - \sigma^{\boldsymbol{v}}_d(\tau)}{\sigma^{\boldsymbol{v}}_d(\tau)}$$

is the relative discrepancy for the demographic variance when using $\boldsymbol{c}$ instead of $\boldsymbol{v}$. Hence, in the following derivation we use the demographic variance to express the relative discrepancy for N_{eV}. First, the demographic variance is rewritten as

$$\sigma^2_{d,\boldsymbol{c}}(\tau) = \lambda^{-\tau-1}\sum_{r=0}^{\tau-1}\lambda^r\boldsymbol{v}\boldsymbol{\Sigma}\boldsymbol{v}'$$
$$+\lambda^{-\tau-1}(\boldsymbol{c}-\boldsymbol{v})\sum_{r=0}^{\tau-1}\tilde{\boldsymbol{g}}^r\boldsymbol{\Sigma}\boldsymbol{v}'$$
$$+\lambda^{-\tau-1}\boldsymbol{v}\boldsymbol{\Sigma}\sum_{r=0}^{\tau-1}(\tilde{\boldsymbol{g}}^r)'(\boldsymbol{c}-\boldsymbol{v})'$$
$$+\lambda^{-\tau-1}(\boldsymbol{c}-\boldsymbol{v})\sum_{r=0}^{\tau-1}\lambda^{-r}\tilde{\boldsymbol{g}}^r\boldsymbol{\Sigma}(\tilde{\boldsymbol{g}}^r)'(\boldsymbol{c}-\boldsymbol{v})'$$
$$+(\boldsymbol{c}-\boldsymbol{v})\boldsymbol{V}(\boldsymbol{c}-\boldsymbol{v})' + o(\max(1,\lambda^{-\tau})), \qquad (G.1)$$

which holds for any $\lambda > 0$, with the last term of smaller order than $\max(1, \lambda^{-\tau})$ as $\tau\to\infty$. For the last term we used that

$$\boldsymbol{c}(\boldsymbol{g}^\tau\lambda^{-\tau} - \boldsymbol{I})\boldsymbol{V}(\boldsymbol{g}^\tau\lambda^{-\tau} - \boldsymbol{I})'\boldsymbol{c}'$$
$$= (\boldsymbol{c}-\boldsymbol{v})(\boldsymbol{g}^\tau\lambda^{-\tau} - \boldsymbol{I})\boldsymbol{V}(\boldsymbol{g}^\tau\lambda^{-\tau} - \boldsymbol{I})'(\boldsymbol{c}-\boldsymbol{v})'$$
$$= (\boldsymbol{c}-\boldsymbol{v})(\tilde{\boldsymbol{g}}^\tau\lambda^{-\tau} - \boldsymbol{I})\boldsymbol{V}(\tilde{\boldsymbol{g}}^\tau\lambda^{-\tau} - \boldsymbol{I})'(\boldsymbol{c}-\boldsymbol{v})'$$
$$= (\boldsymbol{c}-\boldsymbol{v})\boldsymbol{V}(\boldsymbol{c}-\boldsymbol{v})' + o(1).$$

The asymptotics of the demographic variance depends on the growth rate and the following analysis is divided into three cases.

Case 1: When $\lambda = 1$, (G.1) simplifies to

$$\sigma^2_{d,\boldsymbol{c}}(\tau) = \tau \boldsymbol{v}\boldsymbol{\Sigma}\boldsymbol{v}' + (\boldsymbol{c}-\boldsymbol{v})\sum_{r=0}^{\tau-1}\tilde{\boldsymbol{g}}^r\boldsymbol{\Sigma}\boldsymbol{v}' + \boldsymbol{v}\boldsymbol{\Sigma}\sum_{r=0}^{\tau-1}(\tilde{\boldsymbol{g}}^r)'(\boldsymbol{c}-\boldsymbol{v})' + (\boldsymbol{c}-\boldsymbol{v})\sum_{r=0}^{\tau-1}\tilde{\boldsymbol{g}}^r\boldsymbol{\Sigma}(\tilde{\boldsymbol{g}}^r)'(\boldsymbol{c}-\boldsymbol{v})' + (\boldsymbol{c}-\boldsymbol{v})\boldsymbol{V}(\boldsymbol{c}-\boldsymbol{v})' + o(1), \tag{G.2}$$

hence, the demographic variance is dominated by the first term in (G.2) and the relative discrepancy (20) is of order $O(\tau^{-1})$, since

$$\lim_{\tau\to\infty}\tau\Delta_{\boldsymbol{c}}(\tau) = -\lim_{\tau\to\infty}\tau\tilde{\Delta}_{\boldsymbol{c}}(\tau) = C \tag{G.3}$$

where

$$-C = \frac{1}{\boldsymbol{v}\boldsymbol{\Sigma}\boldsymbol{v}'}\left((\boldsymbol{c}-\boldsymbol{v})\sum_{r=0}^{\infty}\tilde{\boldsymbol{g}}^r\boldsymbol{\Sigma}\boldsymbol{v}' + \boldsymbol{v}\boldsymbol{\Sigma}\sum_{r=0}^{\infty}(\tilde{\boldsymbol{g}}^r)'(\boldsymbol{c}-\boldsymbol{v})' + (\boldsymbol{c}-\boldsymbol{v})\sum_{r=0}^{\infty}\tilde{\boldsymbol{g}}^r\boldsymbol{\Sigma}(\tilde{\boldsymbol{g}}^r)'(\boldsymbol{c}-\boldsymbol{v})' + (\boldsymbol{c}-\boldsymbol{v})\boldsymbol{V}(\boldsymbol{c}-\boldsymbol{v})'\right).$$

Case 2: When $\lambda > 1$, if we let $\tau \to \infty$ the first term in (G.1) converges to $(\lambda(\lambda-1))^{-1}\boldsymbol{v}\boldsymbol{\Sigma}\boldsymbol{v}' + o(1)$ and the next three sums tend to zero, conditioned on $|\lambda_1|^2 < \lambda$, hence

$$\sigma^2_{d\boldsymbol{c}}(\tau) = \frac{1}{\lambda(\lambda-1)}\boldsymbol{v}\boldsymbol{\Sigma}\boldsymbol{v}' + (\boldsymbol{c}-\boldsymbol{v})\boldsymbol{V}(\boldsymbol{c}-\boldsymbol{v})' + o(1)$$

as $\tau \to \infty$, so that for the relative discrepancy of the demographic variance and the variance effective population size we have

$$\lim_{\tau\to\infty}\tilde{\Delta}_{\boldsymbol{c}}(\tau) = \frac{\lambda(\lambda-1)}{\boldsymbol{v}\boldsymbol{\Sigma}\boldsymbol{v}'}(\boldsymbol{c}-\boldsymbol{v})\boldsymbol{V}(\boldsymbol{c}-\boldsymbol{v})'$$

and

$$\lim_{\tau\to\infty}\Delta_{\boldsymbol{c}}(\tau) = -\frac{\frac{\lambda(\lambda-1)}{\boldsymbol{v}\boldsymbol{\Sigma}\boldsymbol{v}'}(\boldsymbol{c}-\boldsymbol{v})\boldsymbol{V}(\boldsymbol{c}-\boldsymbol{v})'}{1+\frac{\lambda(\lambda-1)}{\boldsymbol{v}\boldsymbol{\Sigma}\boldsymbol{v}'}(\boldsymbol{c}-\boldsymbol{v})\boldsymbol{V}(\boldsymbol{c}-\boldsymbol{v})'}. \tag{G.4}$$

Since $\lambda > 1$, the right hand side of (G.4) is less or equal to zero.

Case 3: When $\lambda < 1$, (G.1) can be rewritten as

$$\sigma^2_{d,\boldsymbol{c}}(\tau) = \frac{1}{(1-\lambda)\lambda}\lambda^{-\tau}(1+o(1))\boldsymbol{v}\boldsymbol{\Sigma}\boldsymbol{v}' + \frac{1}{\lambda}\frac{1}{\lambda^\tau}(\boldsymbol{c}-\boldsymbol{v})\sum_{r=0}^{\tau-1}\tilde{\boldsymbol{g}}^r\boldsymbol{\Sigma}\boldsymbol{v}' + \frac{1}{\lambda}\frac{1}{\lambda^\tau}\boldsymbol{v}\boldsymbol{\Sigma}\sum_{r=0}^{\tau-1}(\tilde{\boldsymbol{g}}^r)'(\boldsymbol{c}-\boldsymbol{v})' + \frac{1}{\lambda}\frac{1}{\lambda^\tau}(\boldsymbol{c}-\boldsymbol{v})\sum_{r=0}^{\tau-1}\lambda^{-r}\tilde{\boldsymbol{g}}^r\boldsymbol{\Sigma}(\tilde{\boldsymbol{g}}^r)'(\boldsymbol{c}-\boldsymbol{v})' + o(\lambda^{-\tau}).$$

Hence, for the relative discrepancy of the demographic variance, we have that

$$\lim_{\tau\to\infty}\tilde{\Delta}_{\boldsymbol{c}}(\tau) = \frac{1-\lambda}{\boldsymbol{v}\boldsymbol{\Sigma}\boldsymbol{v}'}\left((\boldsymbol{c}-\boldsymbol{v})\sum_{r=0}^{\infty}\tilde{\boldsymbol{g}}^r\boldsymbol{\Sigma}\boldsymbol{v}' + \boldsymbol{v}\boldsymbol{\Sigma}\sum_{r=0}^{\infty}(\tilde{\boldsymbol{g}}^r)'(\boldsymbol{c}-\boldsymbol{v})' + (\boldsymbol{c}-\boldsymbol{v})\sum_{r=0}^{\infty}\lambda^{-r}\tilde{\boldsymbol{g}}^r\boldsymbol{\Sigma}(\tilde{\boldsymbol{g}}^r)'(\boldsymbol{c}-\boldsymbol{v})'\right) = -\left(1+\frac{1}{\lim_{\tau\to\infty}\Delta_{\boldsymbol{c}}(\tau)}\right)^{-1}. \quad \square \tag{G.5}$$

References

Allendorf, F.W., England, P.R., Luikart, G., Ritchie, P.A., Ryman, N., 2008. Genetic effects of harvest on wild animal populations. Trends in Ecology & Evolution 23, 327–337.

Allendorf, F.W., Ryman, N., 2002. The role of genetics in population viability analysis. Population Viability Analysis 50–85.

Baker, M., Mewaldt, L., Stewart, R., 1981. Demography of white-crowned sparrows (*Zonotrichia leucophrys nuttalli*). Ecology 62, 636–644.

Caswell, H., 2001. Matrix Population Models: Construction, Analysis, and Interpretation. Sinauer Associates Inc.

Charlesworth, B., 2009. Effective population size and patterns of molecular evolution and variation. Nature Reviews Genetics 10, 195–205.

Collet, P., Nez, S., San Martín, J., 2013. Quasi-Stationary Distributions: Markov Chains. In: Diffusions and Dynamical Systems, Springer.

Connell, J., 1970. A predator–prey system in the marine intertidal region. i. *Balanus glandula* and several predatory species of thais. Ecological Monographs 40, 49–78.

Crow, J., Denniston, C., 1988. Inbreeding and variance effective population numbers. Evolution 482–495.

Crow, J., Kimura, M., 1970. An Introduction to Population Genetics Theory. Burgess Intl. Group.

Darroch, J., Seneta, E., 1965. On quasi-stationary distributions in absorbing discrete-time finite markov chains. Journal of Applied Probability 2, 88–100.

Engen, S., Lande, R., Saether, B., 2005a. Effective size of a fluctuating age-structured population. Genetics 170, 941–954.

Engen, S., Lande, R., Saether, B., Weimerskirch, H., 2005b. Extinction in relation to demographic and environmental stochasticity in age-structured models. Mathematical Biosciences 195, 210–227.

Ewens, W., 2004. Mathematical Population Genetics: I. In: Theoretical Introduction, vol. 27. Springer.

Felsenstein, J., 1971. Inbreeding and variance effective numbers in populations with overlapping generations. Genetics 68, 581–597.

Fisher, R., 1958. The Genetical Theory of Natural Selection, second ed. Dover Publications, Inc., New York.

Franklin, I.R., 1980. Evolutionary change in small populations.

Grimmett, G., Stirzaker, D., 2001. Probability and Random Processes. Oxford University Press, USA.

Hill, W., 1972. Effective size of populations with overlapping generations. Theoretical Population Biology 3, 278–289.

Hill, W., 1979. A note on effective population size with overlapping generations. Genetics 92, 317–322.

Hössjer, O., 2011. Coalescence theory for a general class of structured populations with fast migration. Advances in Applied Probability 43, 1027–1047.

Hössjer, O., Ryman, N., 2013. Quasi equilibrium, variance effective population size and fixation index for models with spatial structure. To appear in Journal of Mathematical Biology.

Jamieson, I.G., Allendorf, F.W., 2012. How does the 50/500 rule apply to mvps? Trends in Ecology & Evolution.

Jorde, P., 2012. Allele frequency covariance among cohorts and its use in estimating effective size of age-structured populations. Molecular Ecology Resources 12, 476–480.

Jorde, P., Ryman, N., 1995. Temporal allele frequency change and estimation of effective size in populations with overlapping generations. Genetics 139, 1077–1090.

Jorde, P., Ryman, N., 1996. Demographic genetics of brown trout (*Salmo trutta*) and estimation of effective population size from temporal change of allele frequencies. Genetics 143, 1369–1381.

Jorde, P., Ryman, N., 2007. Unbiased estimator for genetic drift and effective population size. Genetics 177, 927–935.

Lande, R., Barrowclough, G.F., 1987. Effective Population Size, Genetic Variation, and Their Use in Population Management. Cambridge University Press.

Lande, R., Engen, S., Sæther, B., 2003. Stochastic Population Dynamics in Ecology and Conservation. Oxford University Press, USA.

Lande, R., Orzack, S., 1988. Extinction dynamics of age-structured populations in a fluctuating environment. Proceedings of the National Academy of Sciences 85, 7418–7421.

Leslie, P., 1945. On the use of matrices in certain population mathematics. Biometrika 183–212.

Luikart, G., Cornuet, J., Allendorf, F., 1999. Temporal changes in allele frequencies provide estimates of population bottleneck size. Conservation Biology 13, 523–530.

Nagylaki, T., 1980. The strong-migration limit in geographically structured populations. Journal of Mathematical Biology 9, 101–114.

Nei, M., 1975. Molecular Population Genetics and Evolution, vol. 40. North-Holland.

Nei, M., Tajima, F., 1981. Genetic drift and estimation of effective population size. Genetics 98, 625–640.

Ryman, N., Baccus, R., Reuterwall, C., Smith, M.H., 1981. Effective population size, generation interval, and potential loss of genetic variability in game species under different hunting regimes. Oikos 257–266.

Sæther, B.E., Engen, S., Solberg, E., 2009. Effective size of harvested ungulate populations. Animal Conservation 12, 488–495.

Sagitov, S., Jagers, P., 2005. The coalescent effective size of age-structured populations. The Annals of Applied Probability 15, 1778–1797.

Sjödin, P., Kaj, I., Krone, S., Lascoux, M., Nordborg, M., 2005. On the meaning and existence of an effective population size. Genetics 169, 1061–1070.

Tuljapurkar, S., 1982. Population dynamics in variable environments. ii. correlated environments, sensitivity analysis and dynamics. Theoretical Population Biology 21, 114–140.
Wang, J., Caballero, A., 1999. Developments in predicting the effective size of subdivided populations. Heredity 82, 212–226.
Wang, J., Whitlock, M., 2003. Estimating effective population size and migration rates from genetic samples over space and time. Genetics 163, 429–446.
Waples, R., 1989. Temporal variation in allele frequencies: testing the right hypothesis. Evolution 1236–1251.
Waples, R., 2002. Definition and Estimation of Effective Population Size in the Conservation of Endangered Species. University of Chicago Press.
Waples, R., Yokota, M., 2007. Temporal estimates of effective population size in species with overlapping generations. Genetics 175, 219–233.
Wright, S., 1931. Evolution in mendelian populations. Genetics 16, 98–160.